

Raman Spectra and Electronic Structure of Alkaline Metal Doped Polyacetylene and β -Carotene

Jiro TANAKA,* Yasuyoshi SAITO, Masaaki SHIMIZU, Chizuko TANAKA,
and Masashi TANAKA†

Department of Chemistry, Faculty of Science, Nagoya University,
Chikusa-ku, Nagoya 464

†College of General Education, Nagoya University, Chikusa-ku, Nagoya 464
(Received October 8, 1986)

Raman spectra of alkaline metal doped polyacetylene were studied at various levels of doping for $(\text{CHM}_y)_x$ and $(\text{CDM}_y)_x$, $\text{M}=\text{Na}$ and K , with $y=0-0.18$. Several steps in the doping process can be recognized in changes of the Raman spectra; the initial Raman lines remain for $y=0-0.06$ but change completely into a new pattern at $y=0.13$. Raman and ESR spectra of alkaline metal doped β -carotene were measured as a model study of the alkaline metal doping of polyacetylene. The correlation of these spectra together with the *ab initio* SCF MO calculation on model compounds show that a heavily alkaline metal doped polyacetylene chain does not have a uniform bond length structure but is composed of a charged soliton structure connected by a uniform chain. The new Raman bands were assigned based on this structure, implying that a bond alternation still exists in the metallic state of alkaline doped polyacetylene.

Raman spectra of neat and doped polyacetylene (PA) provide characterizing insight regarding the molecular structure of the polymer.¹⁾ The change in the Raman spectra upon doping the polymer has been extensively investigated; however, only a relatively few studies have appeared which discuss the quantitative aspect of alkaline metal doping of PA.^{2,3)} Recently, Heeger et al.^{4,5)} discussed the structural change from a spinless soliton lattice to a metallic polaron lattice in alkaline metal doping of PA by an ESR measurement. In this paper we present Raman spectral evidence of a structural change occurring at a definite level of Na and K doping of $(\text{CH})_x$ and $(\text{CD})_x$. The Raman and ESR spectra of Na-doped β -carotene were measured; here, the structure of the anion radical is discussed in terms of an analysis of the hyperfine structure and chemical information. The structure of alkaline metal doped PA is considered from an *ab initio* SCF MO calculation of the model compound⁶⁾ and a close similarity of the Raman spectra between the Na doped PA and Na doped β -carotene. The present study gives information regarding the structural aspect of a heavily doped PA lattice and the nature of the structural change occurring in the doping of PA.

Experimental

Materials. Thin films of PA were synthesized by Shirakawa's method⁷⁾ on the inner surface of a quartz cell for UV, visible, near IR and Raman spectral measurements. Doping was carried out by the use of naphthalene anions in a dried THF solution. The film was immersed into the solution under a completely sealed condition and washed with THF for five to ten times until the solution became colorless. β -Carotene was recrystallized from benzene and stored under a nitrogen atmosphere.

Spectrometers. Visible and near IR spectra were measured by a Hitachi model 330 spectrophotometer (4000–4000 cm^{-1}). In situ doping and combined visible, near IR and Raman spectral measurements were carried out using a

JEOL Model JRS 400T spectrometer with Ar-ion (Spectra Physics 164-05) and He-Ne lasers (Spectra Physics 125A) and a Varian Model 2300 spectrophotometer at the Instrument Center of Institute for Molecular Science (IMS). ESR spectra were obtained by a Varian E112 at X-band in IMS. IR spectra were measured with a Hitachi 230-50 spectrophotometer.

Analysis. The dopant content was analyzed by a flame analysis using an Evans Model 100 flame photometer. A radiation chemical analysis was performed with some films by Dr. Tohru Kishi of National Police Science Institute.

Conductivity. All conductivity measurements were carried out by a four-probe technique, and the mechanical pressed contacts were applied between the film and the Pt leads. The measurement was carried out down to 80 K in cold N_2 gas.

Results and Discussion

(1) Doping and Electronic Spectra. The visible and near IR spectra of PA are largely dependent on the concentration of the dopant in PA.^{8–10)} In order to estimate the doping level of the polymer, the visible and near IR absorption of Na-doped PA were measured at several concentrations of the dopant. The spectra were taken on different films of approximately the same thickness; the absorbance was recorded by normalizing the absorption peak of *cis*-PA at 18500 cm^{-1} to unity. The change in the spectra upon doping in the near IR region was recorded with reference to the peak intensity of an undoped *cis*-rich film. The dopant content was analyzed on each thin film; the thickness of the film was estimated before doping by the absorption intensity¹¹⁾ and the total amount of PA was determined from the area and the thickness of the film. Then, the composition was determined on each film. The optical densities of the doped film were found to change with the dopant concentration.¹⁰⁾ It appears that the 6000 cm^{-1} band increases almost linearly, while the 18500 cm^{-1} band

also decreases linearly with the dopant concentration. A change in the spectra might be recognized as being due to a transition from the undoped cis-(CH)_x to the doped state of PA. A doped film has a characteristic electronic absorption band at about the 6000 cm^{-1} region.⁸⁾ Another broad peak was recognized around the 38000 cm^{-1} region, which may indicate that the electronic structure of the polyene chain is completely changed. By the use of a linear relation¹⁰⁾ between the dopant concentration and the absorption intensities, the dopant level was estimated for each doped film in the following measurements. The ratio of the optical densities in the near IR region to the maximum in the visible region before the doping was used to estimate the dopant concentration at each stage of doping.

The change in the electronic spectra after compensation of the dopant by H_2O in the air is shown in Fig. 1. The spectrum of the cis-rich film before Na doping is shown by curve 0 and curve 1 is that of a heavily doped film. The vacuum system was leaked to 0.1 Torr (1 Torr=133.322 Pa) and the spectral change was recorded. The intensity of the 6000 cm^{-1} peak decreased and the 16000 cm^{-1} band increased by a reaction of the Na doped film with H_2O . After three hours the intensity at 6000 cm^{-1} almost disappeared and a new peak of the trans form was found at 16000 cm^{-1} ; the cis-form band was not found. The result indicated that the cis-trans isomerization occurred completely by Na doping and that the trans film was obtained by a reaction of Na with H_2O . A side reaction, such as bond cleavage, was not involved since the spectral curve 7 (Fig. 1) was coincident with that of native trans film.

The origin of the 6000 cm^{-1} band is not unique; at the initial stage of doping, the so-called mid gap absorption was found in this region.⁸⁾ However, a

heavily doped film may show broad absorption due to free carriers, as was observed in the case of an I_2 doped PA film.¹²⁾ A distinction between the two origins is not easy; however, the predominance of the mid gap band in the initial stage and the free carrier in the final stage was confirmed by reflectivity measurements as well.⁹⁾

(2) Near IR and Raman Spectra of Doped trans-(CH)_x . Measurements of near IR absorption and Raman spectra of doped PA films were carried out systematically with in situ doping and monitoring of

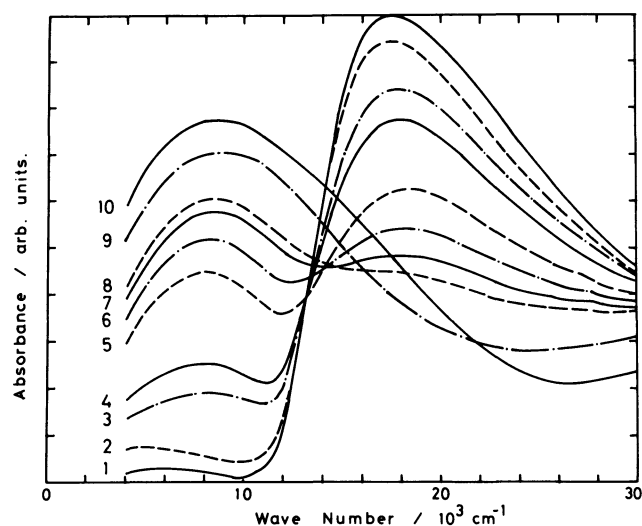


Fig. 2. Absorption spectra of the same thin trans-PA film doped with Na. The numbers of the curves correspond to the doping level γ in $(\text{CHNa}_\gamma)_x$; (1) $\gamma=0$, (2) $\gamma=0.015$, (3) $\gamma=0.036$, (4) $\gamma=0.047$, (5) $\gamma=0.085$, (6) $\gamma=0.095$, (7) $\gamma=0.108$, (8) $\gamma=0.114$, (9) $\gamma=0.133$, and (10) $\gamma=0.146$.

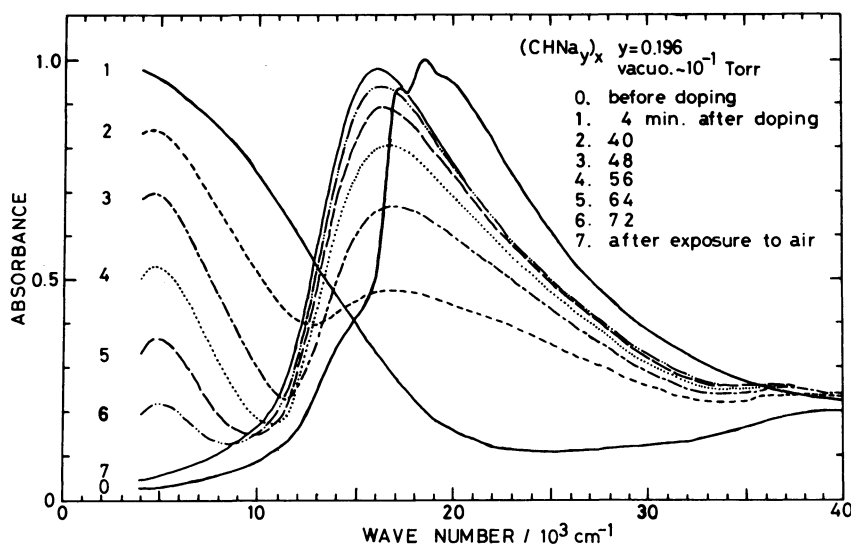


Fig. 1. Absorption spectral change of Na doped as grown $(\text{CH})_x$ film after exposing to the leak of air. (0) undoped film, (1) doped film, after 4 min, (2) 40 min, (3) 48 min, (4) 56 min, (5) 64 min, (6) 72 min, (7) 3 h. exposing to the air.

the dopant level. Figure 2 illustrates changes in the near IR spectra of *trans*-(CH)_x film upon Na doping at each stage; cruve 1 is for undoped *trans*-PA and 10 is for heavily doped film. Two isosbestic points were found in the series of spectra; the first one appears at 13200 cm⁻¹ in the initial stage ($y=0-0.05$; y refers to atomic composition in (CHNa_y)_x) and the second one was observed at 14000 cm⁻¹ in the intermediate stage ($y=0.08-0.11$). The same PA film was used for all measurements. These isosbestic points could be clearly found for initially isomerized *trans*-film; if we use a *cis*-rich film, the *cis*-*trans* isomerization process is involved which shows another spectral change. The

appearance of two distinct isosbestic points may imply that the doping proceeds through several steps, and that it is consistent with electrochemical doping results,¹³ where several reduction potentials were observed for the doping process of $y=0-0.18$.

The Raman spectra measured at 632.8 nm (15803 cm⁻¹) excitation are shown in Fig. 3, where the excitation wavelength is selected so as to obtain optimum efficiencies to both the undoped and doped part of PA. The undoped part showed an absorption peak at 18500 cm⁻¹. On the other hand, the doped part displayed an absorption peak at 6000 cm⁻¹, only a post resonance condition is realized by 15803 cm⁻¹ excitation. In spite of this, the excitation at 632.8 nm is the best means to find any structural change during the doping process by the Raman spectra. This is because short-wavelength excitation shows little efficiency to the Raman bands of the doped part of PA.

Figure 3 shows that the characteristic Raman bands of *trans*-PA at 1470 and 1080 cm⁻¹ did not change at all during the initial stage of doping (curves 1-4). In contrast with this, the characteristic absorption band in the near IR region increased linearly with the dopant; therefore, it is suggested that the skeletal conformation of PA is not significantly changed from the initial structure during the first stage of doping except for the local region where Na is coordinated. The structure of the metal coordinated chain is found by a theoretical calculation⁶ (Fig. 4); this particular structure may be called a charged soliton structure in the following discussion. For a light doping level, charged soliton structures are formed in pairs, since no spin susceptibility has been found and such a structure has been called bipolaron.^{8,14} The singlet state is obtained by putting two charged soliton structures at distant positions of the conjugated chain with an inversion symmetry; such a chain may give Raman spectra that are almost the same as that of undoped PA.

In the spectra of an intermediate stage of doping (Fig. 3, curves 5-8), new Raman lines appear at 1560, 1275 cm⁻¹ etc.; however, a reminiscence of the initial lines suggests that the lightly doped bipolaron structure coexists with the new structure at this stage ($0.08 < y < 0.11$). The intensities of the new and initial

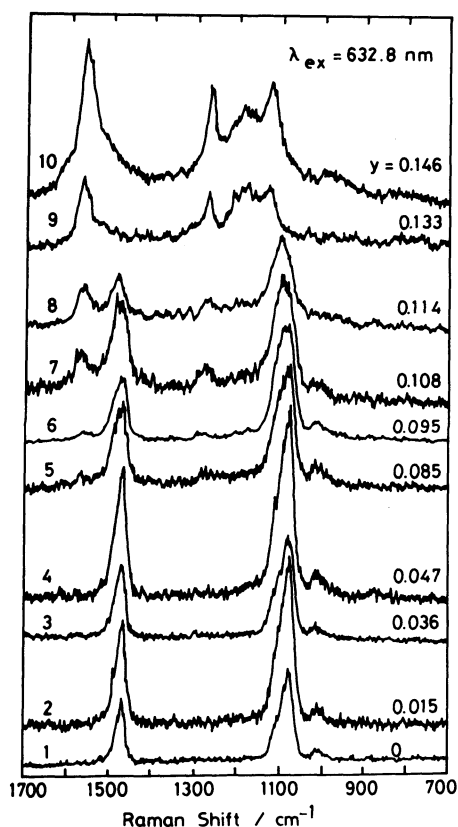


Fig. 3. Raman spectra of thin *trans*-(CH)_x film doped with Na; the composition is shown by the value of y in (CHNa_y)_x.

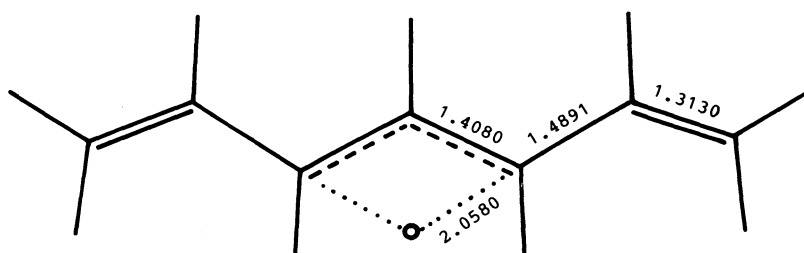


Fig. 4. A model of charged soliton structure, C₇H₉LI, estimated by ab initio SCF MO calculation.

bands are almost equal at $y=0.114$; the spectra changed completely to a new form above $y=0.133$. The new structure shows strong peaks at 1570, 1275, 1180, and 1125 cm^{-1} and weak ones at 1040 and 900 cm^{-1} . The transition to the new form may be completed at $y\approx 0.13$; the critical point to the new form may be at $y=0.12-0.13$.

The changes in the visible, near IR and Raman spectra with K doping were almost the same as that of Na doping. The Raman spectrum of a heavily K-doped $(\text{CH})_x$ film showed a peak at 1560 cm^{-1} , about 10 cm^{-1} lower compared to the Na doped film. This result indicates that the 1560 cm^{-1} band is closely connected with the charged soliton structure, since the position is affected by the kind of coordinated metal atom.

(3) Doping and Spectral Changes of *trans*-(CD)_x. Changes in the visible and near IR spectra of Na doped *trans*-(CD)_x were measured (Fig. 5). The 18500 cm^{-1} band decreased and the 6000 cm^{-1} band increased as the doping proceeded. Isosbestic points were found at 12500 and 14000 cm^{-1} , as detected in $(\text{CH})_x$ film. The dopant level in $(\text{CD})_x$ was similarly estimated as for $(\text{CH})_x$ film using a calibration curve.¹⁰ The change in the Raman spectra with increasing dopant concentration is illustrated in Fig. 6. The critical point of the Raman-spectral change is much clearer for $(\text{CD})_x$ than $(\text{CH})_x$; the Raman band did not change for $y=0-0.09$ (curves 1-4) and the transition state appeared at $y=0.113$ and then changed drastically at $y=0.13$. The transition from the initial state to the new form occurred rather suddenly and the critical concentration was almost same as $(\text{CH})_x$ at $y=0.12$.

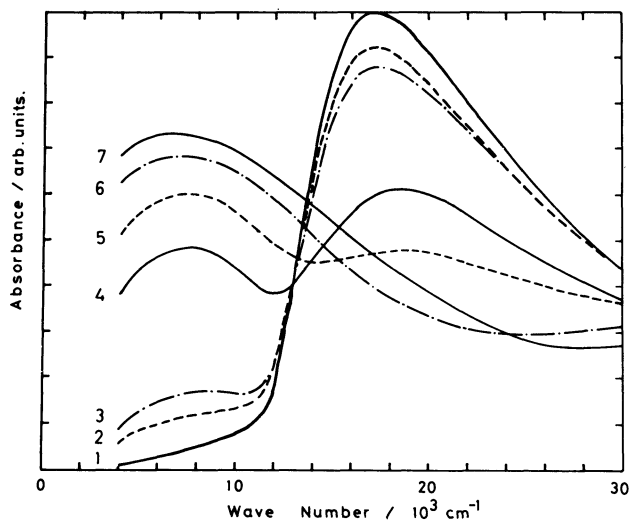


Fig. 5. Absorption spectra of *trans*-(CD)_x film doped with Na. The numbers of absorption curves correspond to the content of Na in $(\text{CDNa}_y)_x$; (1) $y=0$, (2) $y=0.023$, (3) $y=0.031$, (4) $y=0.090$, (5) $y=0.113$, (6) $y=0.129$, and (7) $y=0.140$.

The Raman bands of a heavily K-doped $(\text{CD})_x$ film were found at 1500 and 900 cm^{-1} , which were 20 cm^{-1} lower and 10 cm^{-1} higher than the bands of $(\text{CDNa}_y)_x$. This result is consistent with the previous argument that these bands are associated with the metal coordinated charged soliton region.

(4) Change of Electronic and Raman Spectra in Na Doping of as Grown $(\text{CH})_x$ and $(\text{CD})_x$ Films. An as-grown $(\text{CH})_x$ film by Shirakawa's method is obtained as a cis-rich form but the isomerization to the trans form occurs to some extent at ambient temperature. The Na doping of a cis-rich film accelerates isomerization to the trans form. The Raman spectra may show the process of a cis-trans isomerization and a transformation to the new form. The change in the visible and near IR spectra of a cis-rich film were measured during Na doping; apparent isosbestic points were found at 14300 cm^{-1} for $y=0-0.05$ and at 14800 cm^{-1} for $y=0.08-0.13$. The Raman spectra of the doped cis-rich film were measured and the characteristic cis peaks disappeared almost completely at $y=0.10$; a new peak appeared at $y=0.13$ and a transition to the new form occurred at $y=0.15$ and completed at $y=0.17$. The critical concentration for this transition was relatively higher than the case starting from a pure trans film.

The changes in the Raman spectra of an as-grown $(\text{CD})_x$ film by Na doping were also measured with the

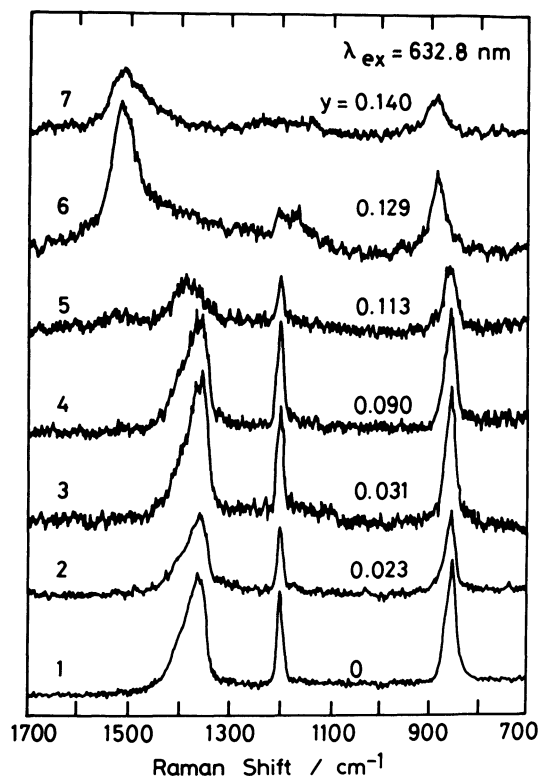


Fig. 6. Raman spectra of *trans*-(CD)_x film doped with Na. The content of Na is shown by y value in the figure.

same film at various stages of doping from $\gamma=0$ to $\gamma=0.18$. The cis-trans isomerization was completed at $\gamma=0.11$ and the new lines were found at $\gamma=0.14$; the transition to the new form was complete at $\gamma=0.18$.

(5) Dispersion of Raman Lines by Changing Excitation Wavelength. The dispersion of the Raman spectra upon changing the excitation wavelength has been found for a *trans*-PA film^{1,15-17}; however, it has been explained by an inhomogeneous distribution of the chain length of the polymer.¹⁷ Dispersion effects were also found for Na-doped ($\gamma=0.11$ and 0.13) and K-doped ($\gamma=0.15$) *trans*-(CH)_x film. The presence of two forms at $\gamma=0.11$ and 0.13 was clearly indicated by changing the excitation wavelength. The film with $\gamma=0.11$ showed only initial PA lines upon 488.0 and 514.5 nm excitations since the content of the new form was too small. The film with $\gamma=0.13$ showed a new band by 632.8 nm excitation and the initial band which was at 1520 cm⁻¹ (514.5 nm) and 1525 cm⁻¹ (488.0 nm excitation), considerably higher than the initial PA band. The completely transformed film with $\gamma=0.15$ showed no initial lines, even upon short wavelength excitation. A slight dispersion of the 1555 cm⁻¹ line was found at 1585 cm⁻¹ (514.5 nm) and 1590 cm⁻¹ (488.0 nm).

The dispersion effect was also measured for the film with $\gamma=0.13$ of *trans*-(CDNa_y)_x and $\gamma=0.18$ of initially cis film. Upon short wavelength excitation of $\gamma=0.13$

film, the 1450 cm⁻¹ band of a relatively short conjugated double bond was found to be rather strong; however, under 632.8 nm excitation the same film exhibited only Raman lines of the new form. In contrast, the heaviest doped film showed only the new lines under excitation at any wavelength, implying that the PA chain was completely transformed into the new form. The Raman lines showed a dispersion effect upon changing the excitation wavelength: 1555 cm⁻¹ (457.9 nm), 1541 cm⁻¹ (514.5 nm), and 1515 cm⁻¹ (632.8 nm), respectively.

The dispersion relation upon changing the excitation wavelength for $\gamma=0.11$ as-grown film was almost the same as that of the undoped *trans* film. However, those for the $\gamma=0.17$ as-grown film showed almost a new form; but a small fraction of the *trans* form was observed under 457.9 nm excitation. The completely transformed as-grown (CDNa_y)_x film ($\gamma=0.18$) showed a small dispersion effect upon changing the excitation wavelength.

(6) DC Conductivity Measurement of Na Doped as Grown (CH)_x. The room-temperature d.c. conductivity of a Na doped as-grown PA film was measured as a function of γ . The conductivity increased rapidly from $\gamma=0$ to 0.03 and saturated at about $\gamma=0.10$. The maximum conductivity was 72 S cm⁻¹ at 295 K for a film with $\gamma=0.18$. The temperature dependence of the conductivity was measured and plotted for $1/T$ (Fig.

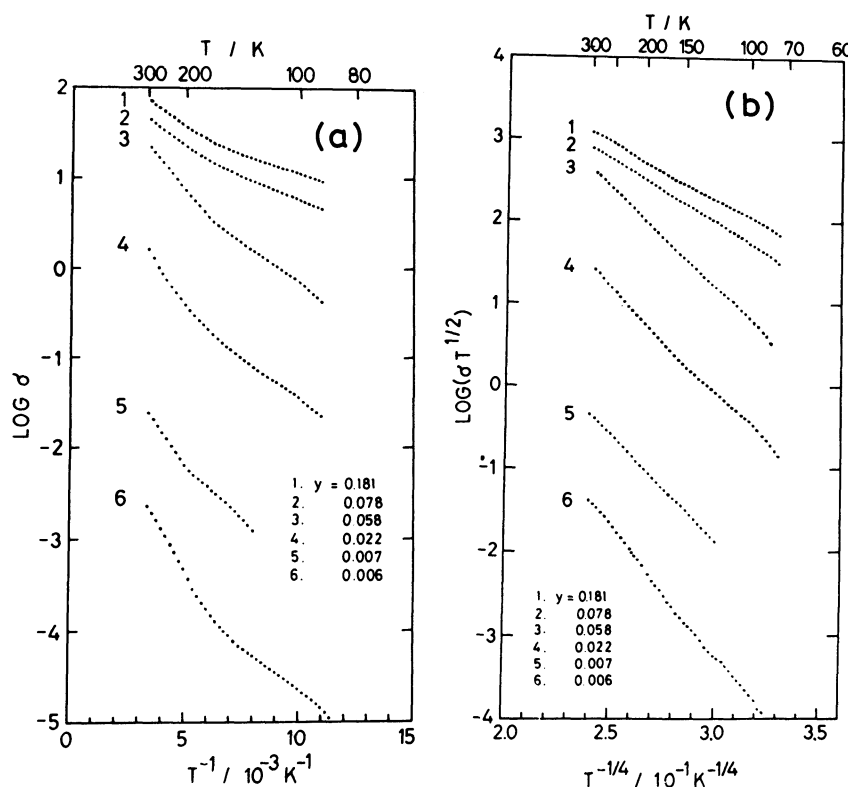


Fig. 7. Temperature dependence of conductivity of Na doped (CH)_x; (a) $\log \sigma$ plot for $1/T$, (b) $\log \sigma T^{1/2}$ plot for $T^{-1/4}$; the doping levels are shown in the figure.

7(a)). Also, the activation energies were estimated from the initial slopes; the values were about 0.1 eV

for lightly doped films and 0.03 eV for $\gamma=0.18$. A plot of $\log(\sigma T^{1/2})$ against $T^{-1/4}$ gave a straight line (Fig. 7(b)). Mott's variable range hopping model¹⁸⁾ could be applied for an analysis of the conduction mechanism. The parameters by this analysis are shown in Table 1, where $T_0=16\alpha^3/k_B N(E_F)$ and α^{-1} is the decay length of a localized state. These values are comparable to the values reported for I_2 and $FeCl_3$ doped $(CH)_x$.^{19,20)}

(7) **Electronic, ESR and Raman Spectra of Na Doped β -Carotene.** The characteristic absorption spectra of β -carotene in the visible region was changed upon Na doping (Fig. 8). As the doping proceeded the absorption band around 20000 cm^{-1} decreased and

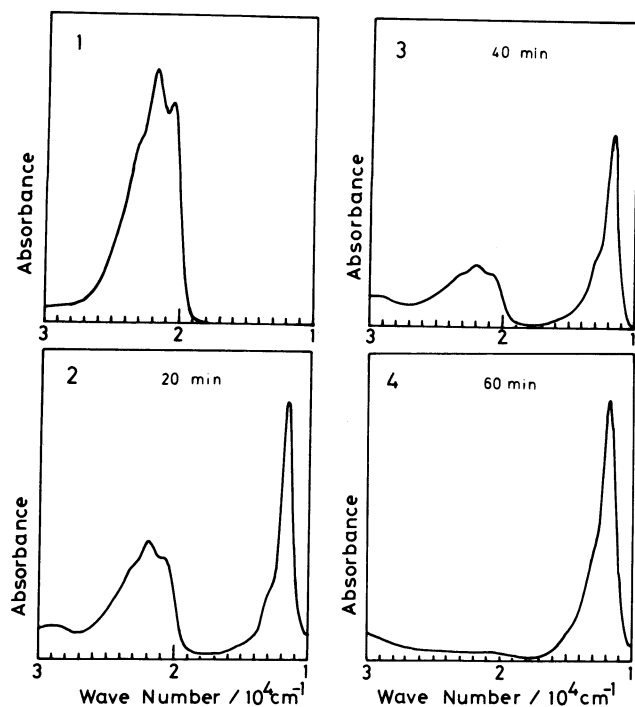


Fig. 8. Absorption spectral changes of β -carotene with Na doping. (1) undoped β -carotene, (2) 20 min, (3) 40 min, (4) 60 min, after doping. (Absorbances are given in arbitrary unit).

Table 1. Parameters for Mott's Variable Range Hopping Model

γ	$\sigma(300^\circ\text{K})/\text{S}\cdot\text{cm}^{-1}$	$T_0/10^6\text{ K}^\circ$	$A/10^7\text{ S}\cdot\text{cm}^{-1}\cdot\text{K}^{1/2}$
0.181	72	1.2	0.34
0.076	44	1.5	0.38
0.056	22	12	62
0.022	1.7	15	7.5
0.010	0.045	40	20
0.006	0.002	46	2.0

The conductivity σ is given by a formula

$$\sigma(T) = AT^{-1/2} \exp(-(T_0/T)^{1/4}), \text{ and}$$

$$A = 0.39(N(E_F)/\alpha k_B)^{1/2} \nu_0 e^2$$

where ν_0 is optical phonon frequency.

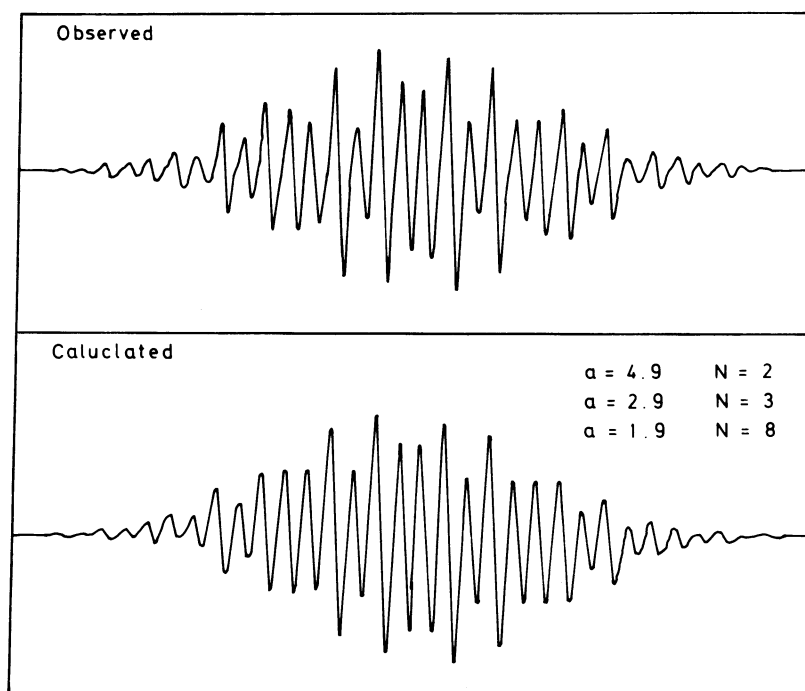


Fig. 9. ESR spectra of Na doped β -carotene in THF solution. Upper curve is the observed ESR spectra by low resolution and the lower one is simulated ESR spectra.

new bands were found at around 12000 cm^{-1} as well as another broad one at a higher energy region. The tail of the higher energy band was found around 30000 cm^{-1} . The ESR spectra of Na-doped β -carotene in a THF solution at low and high resolution were measured (Fig. 9(a)) and the low-resolution spectra were simulated (Fig. 9(b)) by the following coupling parameters: two protons with $a_H=4.9$ Gauss, three protons with $a_H=2.9$ Gauss and eight protons with $a_H=1.9$ Gauss. The agreement between the calculated and the observed spectra are quite satisfactory. In these simulations, the ESR hyperfine structures could be explained by assuming the coupling of an unpaired electron with thirteen hydrogen atoms; this result is important when considering the structure of Na-doped β -carotene.

In order to determine the structure of doped β -carotene, the reaction product of β -carotene with Na was decomposed with H_2O ; also, a mass spectral analysis was performed on the product. It showed that eight hydrogen atoms reacted and that the positions of the coordinated alkaline atoms were guessed (Fig. 10(a)) since the mass spectra indicated a fragmentation of the hydrogenated compound at these positions. This part of the experiment was carried out by Mr. H. Ozeki under the guidance of Dr. M. Kitamura of Prof. Noyori's laboratory. The electrochemical reduction potentials of β -carotene in the THF solution also indicated that the reaction took place to the level of a four-electron reduction.²¹⁾ Then, the structure of the radical, which was found in THF solution, is considered as shown in Fig. 10 (b); the localization of the unpaired electron over the chain of nine carbon atoms can be naturally understood by this structure.

The Raman spectra of Na doped β -carotene in a THF solution were significantly changed by the wavelength of excitation (Fig. 11). This result implies that the solution includes both forms shown in Fig. 10

(a) and (b) and that a doped molecule has several chromophoric groups. The Raman spectrum at 457.9 nm excitation was compared with that of the

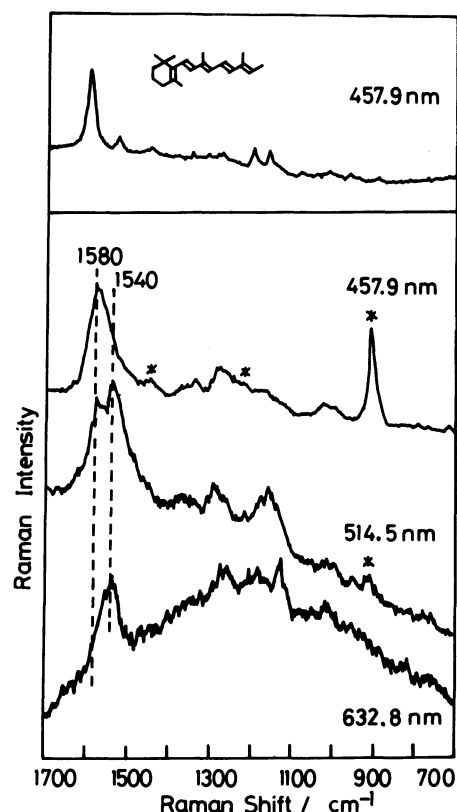


Fig. 11. Raman spectra of Na doped β -carotene and axerophthen. The top curve is that of axerophthen and the upper one is that of Na doped β -carotene, which are excited by 457.9 nm . The middle curve and the bottom one are Raman spectra of Na doped β -carotene excited by 514.5 and 632.8 nm , respectively.

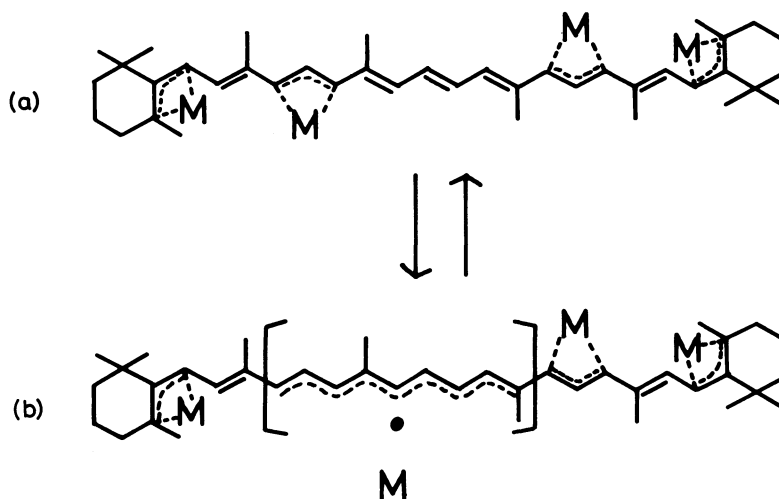


Fig. 10. Equilibrium structures of alkaline metal doped β -carotene.

model compound, axerophthen²², which was kindly prepared by Prof. K. Yamada and Mr. H. Kigoshi of this Department (Fig. 11). The similarity between the two spectra strongly suggests that the doped β -carotene has a partial structure of a short conjugated chain. Regarding SO_2 doping of β -carotene, Harada et al.¹⁾ proposed that the molecule has a shortened double bond system, which is consistent with the present result. By considering these experimental results, the molecular structure of Na-doped β -carotene could be guessed by a formula (a) (Fig. 10).

(8) Structure of Alkaline Metal Doped Polyacetylene. Although a PA film comprises many fibrils and a lightly doped film is never homogeneous, alkaline metal doping proceeds through several stages, implying that a definite conformation exists for each doping step. From the present result and electrochemical studies,¹³⁾ three stages are conceivable for the doping process. When the dopant concentration is dilute ($y < 0.06$), the doped PA chain can have a charged soliton structure (Fig. 12(a)) in which a bipolaron with about twenty carbon atoms between metal atoms can be formed at first. At a higher dopant level, the PA chain has one Na atom for about six carbon atoms ($y = 0.16$) and the chain has unpaired electrons. (Fig. 12(b)) In the intermediate regime ($y = 0.06 - 0.12$) both forms can coexist.

The result of an *ab initio* SCF MO calculation on the model compound, dilitiopolyenes,⁹⁾ is useful for determining the structures of a bipolaron and a heavily doped PA chain. The structure of the singlet state of dilitiopolyene represents a model of the bipolaron structure (Fig. 12(a)). The triplet state has a unique structure in which a charged soliton structure and a chain without bond alternation are sequentially connected (Fig. 12(b)). Such a structural characteristic was already envisaged in the proposed model of β -carotene anion radical, in which the

radical chain is conjugated with a charged soliton structure.

A structural feature of the charged soliton calculated by *ab initio* SCF MO is represented in Fig. 4; one Li atom coordinates to the end two carbon atoms in a three-carbon chain, the bond alternation being lost in the central coordination region which has an intermediate bond length with weak adjacent bonds. Then, the next adjoining bonds are strong (bond lengths are long and short). The planarity of the conjugated chain including the CH bond is lost; the effect of coordination is rather limited within the region shown in Fig. 4. The coordinated Li atom forms a domain wall separating the conjugated chain into regions of different phases. Such a characteristic structure of a charged soliton is always found in both the singlet and triplet states of dilitiopolyene and the doublet state of lithiopolyene. In the singlet state such structures are connected by the normal conjugated double bond with an inversion symmetry in the center of the chain and the conjugation between the soliton structure is extended for long range (Fig. 12(a)). This reduces the Raman frequencies to the value of the extended long chain. In the triplet state the charged soliton structures are connected by a uniform bond length chain and the conjugation between the double-bond units are lost (Fig. 12(b)). This difference in conjugation mode is the origin of a drastic change in the Raman spectra from the initial to the final doped level and in magnetic properties during doping. In the intermediate stage of doping, both structural characteristics can coexist, rather than another structure being involved. This is because the Raman spectra exhibit only the mixed bands of the initial and the final structures (Figs. 3 and 6).

(9) Assignment of Vibrational Bands. The neat *trans*-PA has an alternating double bond structure; the double and single bond lengths are estimated as 1.36

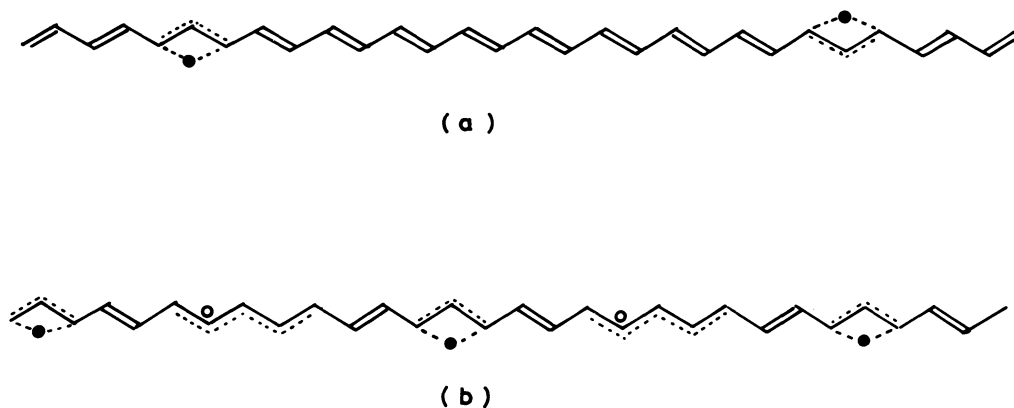


Fig. 12. Proposed model structures of (a) the lightly doped chain (charged soliton pair (bipolaron)) and (b) the heavily doped *trans*-PA chain. The filled circle (●) represents the coordinated alkaline metal ion, and the open circle (○) implies the coordinated alkaline metal atom.

and 1.44 Å, respectively.²³⁾ A normal coordinate analysis on Raman bands of *trans*-PA was recently presented by Takeuchi et al.;²⁴⁾ the 1470 cm^{-1} band and 1079 cm^{-1} band of $(\text{CH})_x$ were assigned to the coupled modes of the $-(\text{C}=\text{C})-$ stretching and the C-H in plane bending and the weak band at 1295 cm^{-1} was assigned to the stretching of the $-(\text{C}-\text{C})-$ single bond.

In the lightly doped *trans*-PA chain, a pair of soliton structures (bipolaron) were formed (Fig. 12(a)); this particular structure may have characteristic IR and Raman bands. In the IR spectra of Na-doped PA reported by Francois et al.²⁵⁾ an intense band was observed at 1410 cm^{-1} , weak bands at 1250 cm^{-1} , and broad strong bands below 1100 cm^{-1} . In the IR spectra of Li-doped PA measured by us (Fig. 13), strong peaks were found at 1420 cm^{-1} , a weak one at 1250–1280 cm^{-1} , another weak one at 1160 cm^{-1} , and fairly strong bands below 1060 cm^{-1} at 1060, 950, 830, and 650 cm^{-1} . These band characteristics are common to the n- and p-doped PA;⁸⁾ therefore, they may be regarded as the charged soliton characteristic band.

The IR absorption bands associated with the charged soliton are not a simple atomic vibration in the usual sense; this is because the atomic vibration is strongly coupled with the charge flow along the chain and the intensities are extraordinarily large compared to usual infrared absorption of the polymer. In the theoretical treatment of the IR absorption of charged soliton by Horovitz²⁶⁾, Wada and Terai et al.,²⁷⁾ and Mele and Hicks²⁸⁾ several in-plane vibrational modes were considered to couple with electron. We suppose that the CH bending and several C-C stretching vibrations around the metal coordinated center are coupled. The prominent IR band at 1400 cm^{-1} is assigned to the C-H in plane bending of the charged soliton structure, because it is largely shifted by deuteration^{29,30)} and the peak position is dependent on the metal species. The weak 1250–1280 cm^{-1} IR band may be the coupled mode of several C-C stretchings around the charged soliton and the strong band

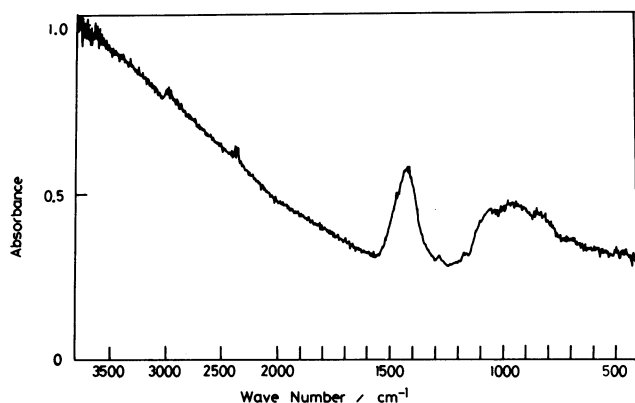


Fig. 13. Infrared spectrum of Li doped thin $(\text{CH})_x$ film.

around 1050 cm^{-1} region may be another coupled mode of C-C stretchings.

The Raman spectra of the lightly or medium doped $(\text{CH})_x$ and $(\text{CD})_x$ did not show any characteristic band of the charged soliton. This is because the electronic absorption band of the charged soliton lies in the near IR region and the resonance condition is not satisfied even under 632.8 nm excitation. Also, the short double bonds in the charged soliton structure are conjugated with the chain of a double-bond system in the bipolaron structure; it may give the vibrational mode of the long chain. In the heavily doped regime, the charged soliton structure is rather isolated (Fig. 12(b)) and the Raman bands of the charged soliton may be found at 1570 and 1125 cm^{-1} in addition to the 1270 and 1180 cm^{-1} bands.

Zannoni and Zerbi³¹⁾ discussed the vibrational modes of doped PA from a symmetry consideration regarding defect structure and a selection rule. They argued that a C_{2v} local symmetry of the charged soliton is rather unlikely compared to the centrosymmetrical defect structure of C_{2h} symmetry. In our analysis, the charged soliton structures might have appeared in pairs by forming a bipolaron during the

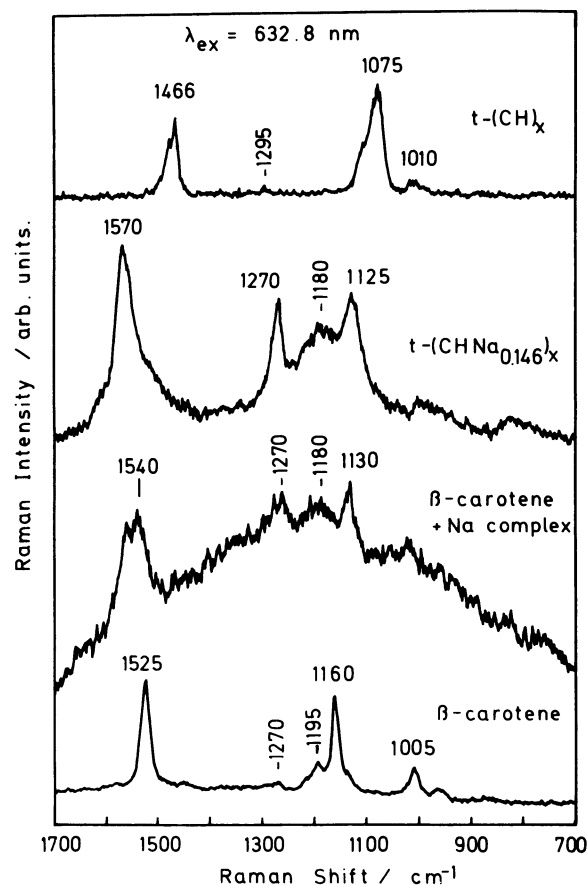


Fig. 14. Comparison of Raman spectra of *trans*- $(\text{CH})_x$, the Na doped film and doped and undoped β -carotene.

early stage of doping; therefore, a center of symmetry is expected in the middle of the conjugated chain and the mutual exclusion of IR and Raman bands may be reasonably understood.

The Raman spectra of a heavily doped $(\text{CH})_x$ film showed a drastically different behavior: $-(\text{C}=\text{C})-$ double bond stretching appeared at a higher frequency (1570 cm^{-1}) and CH bending also shifted to the higher side (1125 cm^{-1}). Also, strong Raman bands could be observed at 1270 and 1180 cm^{-1} ; the former may be associated with $-(\text{C}-\text{C}-\text{C})-$ stretching in the center of the charged soliton structure and the broad 1180 cm^{-1} band may be the stretching of the $-(\text{C}-\text{C}-\text{C})-$ bond in the uniform bond chain. Both bands could be weakly observed in the IR spectra of Li doped PA (Fig. 13). This result is consistent with the selection rule, since an inversion symmetry is lost in the triplet chain model shown in Fig. 12(b) and a local symmetry of C_{2v} may be valid. The observed high-frequency shift can be reasonably explained by the model structure of triplet dilithiopolyene (Fig. 12(b)), where the short double bonds are connected with a uniform chain. In this conformation the conjugation with another double-bond system is interrupted. Takeuchi et al.²⁴ discussed the relationship between the $-(\text{C}=\text{C})_n-$ stretching frequency and the number of double bond units n in a neutral trans-polyene chain. Following their calculation, the observed Raman band at 1540 cm^{-1} in heavily doped PA corresponds reasonably to the ethylenic double bond (Fig. 12(b)).

The similarity of Raman spectra for heavily Na doped *trans*-PA and Na doped β -carotene excited by 632.8 nm is very remarkable when compared it in the same chart (Fig. 14). Skeletal vibrations of $-(\text{C}=\text{C})-$ bonds and CH bending modes were found at almost the same position in both spectra; also, the positions of new $-(\text{C}-\text{C}-\text{C})-$ modes were also the same. Such a close agreement might be explained only when similar backbone structures are involved. The structures of Na doped β -carotene shown in Fig. 11 have an isolated butadiene or ethylene-type skeletons and the uniform radical type chain, and these characteristics are also apparent in the model structure of Fig. 12(b). Following the calculation of Takeuchi et al.²⁴ the 1580 cm^{-1} band in doped β -carotene might be related to the butadiene or hexatriene skeletons. The observed band positions by 457.9 and 632.8 nm excitation may correspond to butadiene and ethylene type bonds; the observed values are in good agreement with their calculation.

The Raman and IR spectra of Na, K, and Li doped PA at various levels of doping showed that a characteristic structural change from the charged soliton lattice to the new structure occurred in the heavily doped regime. The new structure comprised both charged soliton and the uniform chain units.

The structural transformation observed by Raman spectra is in accordance with electrochemical results¹³ and ESR experiments.^{4,5}

A transition to the new structure started at about $y \approx 0.08$, and was completed at about $y \approx 0.13$ level in $(\text{CH})_x$; this is in partial agreement with ESR results.^{4,5} It occurred rather sharply at $y = 0.11$ in $(\text{CD})_x$. A simple model of a one-dimensional metal of uniform bond was not substantiated in the present analysis since the Raman spectra of a heavily doped film showed a pattern of isolated short double bonds. In the Raman spectra of the polymethine cyanine dye³² studied in this laboratory, the skeletal stretching mode of the uniform $-(\text{C}-\text{C}-\text{C})-$ bond was found at the 1300 cm^{-1} region; this may correspond to the 1280 cm^{-1} band in heavily doped PA. A theory of a polaron metal was presented by Kivelson and Heeger,³³ however, a structural view regarding the polaron lattice was not clearly described. The present structure may afford a model of the regular polaron lattice which was considered in their treatment.

The most important consequence of the present result is that the heavily doped chain is composed of a twill unit comprising a charged soliton structure and a uniform chain unit in an alternating sequential way. Further investigation concerning other aspects of the structure may be required in order to clarify details of the physicochemical properties of doped PA.

All Raman measurements were carried out at the Instrument Center of the Institute for Molecular Science. A part of this study was a joint research program at IMS. We are grateful to the Director General Professor Saburo Nagakura and Professor Iwao Yamazaki for the joint program. A part of this work was supported by a grant in aid of the Ministry of Education (No. 61103003) for organic thin films for information conversion. We also thank Professors Ryoji Noyori and Kiyoyuki Yamada and Dr. Masato Kitamura, Messrs. Hideo Kigoshi and Hiroyuki Ozeki for their help during the experiment and to Dr. Tohru Kishi of the Institute of National Police Science for the radiation chemical analysis.

References

- 1) I. Harada, Y. Furukawa, M. Tasumi, H. Shirakawa, and S. Ikeda, *J. Chem. Phys.*, **73**, 4746 (1980); Y. Furukawa, I. Harada, M. Tasumi, H. Shirakawa, and S. Ikeda, *Chem. Lett.*, **1981** 1489.
- 2) E. Faulques, F. Rachdi, S. Lefrant, and P. Bernier, *Synth. Metals*, **9**, 53 (1984).
- 3) H. Eckhardt, L. W. Shacklette, J. S. Szobota, and R. H. Baughman, *Mol. Cryst. Liq. Cryst.*, **117**, 401 (1985).
- 4) J. Chen, T.-C. Chung, F. Moraes, and A. J. Heeger, *Solid State Commun.*, **53**, 757 (1985).
- 5) T. C.-Chung, F. Moraes, J. D. Flood, and A. J. Heeger, *Phys. Rev. B*, **29**, 2341 (1984).

- 6) C. Tanaka, J. Tanaka, and K. Hirao, to be published.
 - 7) H. Shirakawa and S. Ikeda, *Polym. J.*, **2**, 231 (1971).
 - 8) J. Tanaka and M. Tanaka, "Handbook of Conducting Polymers," ed by T. A. Skotheim, Marcel Dekker, New York (1986) Vol. 2, p. 1269.
 - 9) J. Tanaka, K. Kamiya, M. Shimizu, and M. Tanaka, *Synth. Metals*, **13**, 177 (1986).
 - 10) J. Tanaka, M. Tanaka, H. Fujimoto, K. Kamiya, Y. Saito, and T. Kishi, *Mol. Cryst. Liq. Cryst.*, **117**, 259 (1985).
 - 11) H. Fujimoto, K. Kamiya, J. Tanaka, and M. Tanaka, *Synth. Metals*, **10**, 367 (1985).
 - 12) H. Fujimoto, J. Tanaka, M. Tanaka and T. Kishi, *Synth. Metals*, **16**, 133 (1986).
 - 13) L. W. Shacklette and J. E. Toth, *Phys. Rev. B*, **32**, 5892 (1985).
 - 14) J. L. Bredas, *Mol. Cryst. Liq. Cryst.*, **118**, 49 (1985); J. L. Bredas and G. B. Street, *Acc. Chem. Res.*, **18**, 309 (1985). Bredas did not use a terminology of bipolaron for a pair of charged soliton in PA because of degenerate ground state of undoped PA. However, if we coordinate the dopant rather strongly to the chain, the degeneracy might be lost and the chain with a pair of charged soliton may be called as a bipolaron.
 - 15) H. Kuzmany, *Phys. Stat. Sol. (b)*, **97**, 521 (1980).
 - 16) D. B. Fitch, *Mol. Cryst. Liq. Cryst.*, **83**, 95 (1982).
 - 17) R. Tubino, *Mol. Cryst. Liq. Cryst.*, **117**, 319 (1985).
 - 18) N. F. Mott and E. A. Davis, "Electronic Processes in Non-Crystalline Materials," (Clarendon, Oxford) (1979).
 - 19) A. J. Epstein, H. Rommelmann, R. Bigelow, H. W. Gibson, D. M. Hoffmann, and D. B. Tanner, *Phys. Rev. Lett.*, **50**, 1866 (1983).
 - 20) M. Przybylski, B. R. Bulka, I. Kulszewics, and A. Pron, *Solid State Commun.*, **48**, 893 (1983).
 - 21) V. G. Mairanovsky, A. A. Engovatov, N. T. Ioffe, and G. I. Samokhvalov, *J. Electroanal. Chem.*, **66**, 123 (1975); S. M. Park, *J. Electrochem. Soc.*, **125**, 216 (1978).
 - 22) P. Karrer and J. Benz, *Helv. Chim. Acta*, **31**, 1048 (1948).
 - 23) J. P. Pouget, P. Robin, R. Comes, H. W. Gibson, A. J. Epstein, and D. Billaud, *Physica*, **127B**, 158 (1984).
 - 24) H. Takeuchi, Y. Furukawa, I. Harada, and H. Shirakawa, *J. Chem. Phys.*, **84**, 2882 (1986).
 - 25) B. Francois, M. Bernard, and J. J. Andre, *J. Chem. Phys.*, **75**, 4142 (1981).
 - 26) B. Horowitz, *Solid State Commun.*, **41**, 729 (1982).
 - 27) A. Terai, H. Ito, Y. Ono, and Y. Wada, *J. Phys. Soc. Jpn.*, **54**, 196 (1985); A. Terai, Y. Ono, and Y. Wada, *J. Phys. Soc. Jpn.*, **55**, 2889 (1986).
 - 28) E. J. Mele and J. C. Hicks, *Phys. Rev., B*, **32**, 2703 (1985).
 - 29) H. Fujimoto, M. Tanaka, and J. Tanaka, *Bull. Chem. Soc. Jpn.*, **56**, 671 (1983).
 - 30) H. Takeuchi, Y. Furukawa, I. Harada, and H. Shirakawa, *J. Chem. Phys.*, **80**, 2925 (1984).
 - 31) G. Zannoni and G. Zerbi, *J. Mol. Struct.*, **100**, 505 (1983).
 - 32) M. Sano, M. Shimizu, and J. Tanaka, to be published.
 - 33) S. Kivelson and A. J. Heeger, *Phys. Rev. Lett.*, **55**, 308 (1985).
-